Sensors & Actuators: A. Physical xxx (xxxx) xxx-xxx

Contents lists available at ScienceDirect

Sensors & Actuators: A. Physical

journal homepage: www.elsevier.com

Spatial-frequency multiplexing of high-sensitivity liquid level sensors based on multimode interference micro-fibers

Marko Galarza *, Rosa Ana Perez-Herrera , Daniel Leandro , Aitor Judez , Manuel López-Amo

Universidad Pública de Navarra, Dept. of Electrical, Electronic and Communication Engineering and Institute of Smart Cities, Campus Arrosadía, 31006, Pamplona, Spain

ARTICLE INFO

Article history:
Received 13 August 2019
Received in revised form 19 March 2020
Accepted 24 March 2020
Available online xxx

Keywords:
Frequency division multiplexing
Level control
Optical fiber applications
Optical fiber sensors

ABSTRACT

This paper shows a new fiber optic sensor multiplexed system for liquid level sensing. Biconical fiber tapers converging at a 40 mm-long micro-fiber are used as transducers. The tapers are designed to provide the propagation of the two main cylindrical modes in the micro-fiber avoiding higher order modes or modes with other symmetries. The liquid level is calculated in real time from the measurement of the frequency and phase components of the spectral interference pattern of the submerged micro-fiber. The system is fully characterized by theoretical simulations in terms of the sensitivity as a function of the most responsive parameter, which is the width of the micro-fiber. Phase sensibilities of 3.7 rad/mm are experimentally obtained and values as high as of the micro-fiber 11.4 rad/mm are theoretically predicted. The strong dependence of the spatial frequency with the width of the micro-fiber has been used to multiplex three sensors in series in this domain. The maximum detected crosstalk between sensors is 0.2 rad/mm.

1. Introduction

Nowadays, liquid level sensing is indeed an active investigation field [1,2]. The need of precise level measurements of liquids mainly arises in industrial environments where large volumes of liquids are stored [3]. However, short and high-resolution liquid level sensors are also required for minor containers in industrial areas such as medicine, biology [4] and even electronics manufacturing [5]. The market offers a wide variety of devices that base their functionality on many other technologies such as ultrasounds [6], capacitors [7], piezoelectric resonance [8], liquid resistance [9] or artificial vision [10]. Optical fiber sensors also join this list because many fiber configurations have been successfully proved for liquid level measurements. Among them, we find Mach-Zehnder interferometers [2,11], Sagnac loops [12], polymer optical fiber Bragg grating (POFBG) [13], or microstructured polymer optical fiber Bragg grating (mPOFBG) [14], D-shape fibers [15], no-core fibers [16], quasi-distributed fibers [17], multipoint pressure sensors [18] or codified fibers for digital applications [19] among others. Depending on the operating principle, these sensor systems show the following drawbacks. Power based sensors experience lower robustness and multiplexing difficulties. The presence of mechanical elements requires lubrication and maintenance of the sensor in order to minimize their deterioration over time. Complex fibers are expensive and difficult to find. Finally, sensors based on distributed measurements require high cost equipment.

Micro-fibers obtained from the biconical tapering of standard single-mode fibers (SMF) are structures widely used as sensors from long time ago [20,21]. Current technology allows the accurate and repetitive fabrication of intermediate long micro-fibers between biconical tapers making such structures suitable for short-range liquid level measurements. Heating and rapidly stretching the fiber, its nominal diameter can be narrowed down to a microwire of a few micrometers receiving the name of down-tapers [2]. Those tapered fiber sensors can be used either in a cascade configuration [22,23] or individually, as we do in this work. Likewise, waist diameter can be enlarged in an up-taper configuration [2], achieving also high sensitivity in liquid level measurement setups [24].

Micro-fibers are strongly confined cylindrical multimode structures defined by the silica waist and the surrounding medium. The incoming taper, properly designed beyond the adiabaticity criterion, provides the excitation of higher order modes in the micro-fiber. The interaction of the modes along the propagation in the fiber provides an interference pattern in the optical spectrum [25]. The Fast Fourier Transform (FFT) of these fringes is calculated in real time [26] in order to obtain their spatial frequency and phase, both parameters being used to calculate the level of the liquid.

In this paper, we present the spatial frequency multiplexing of a system of highly sensitive tapered micro-fibers for different liquid level measurements. Preliminary results were published in OFS 26 [27]. The theoretical design process and simulation calculations are in good agreement with the obtained experimental results, and are also shown in this work.

* Corresponding author at: Universidad Pública de Navarra, Dept. of Electrical, Electronic and Communication Engineering, Campus Arrosadía, 31006, Pamplona, Spain.
Email address: marko.galarza@unavarra.es (M. Galarza)

https://doi.org/10.1016/j.sna.2020.111985
0924-4247/

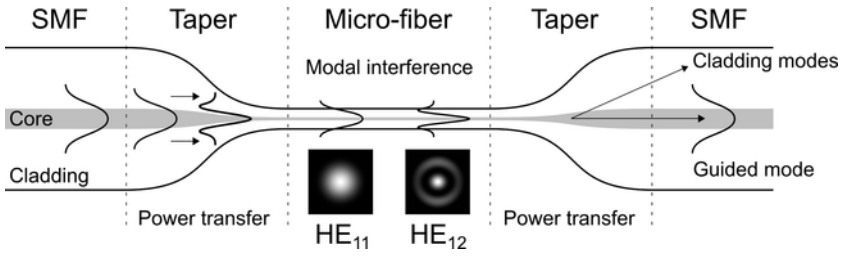

Fig. 1. Schematic of the biconical tapered fiber. Transitions are properly designed in order to provide controlled power transfer between the two main cylindrical modes in the micro-fiber. These modes undergo variable interference patterns depending on the external conditions that influence their propagation constants.

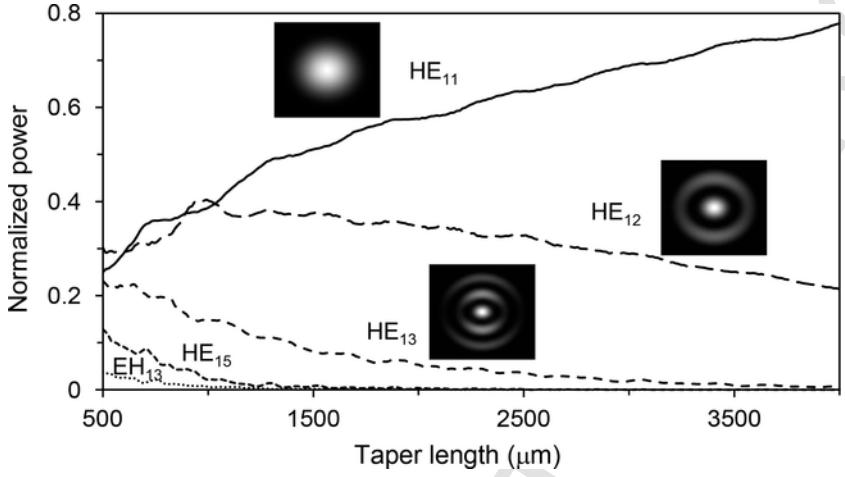

Fig. 2. Calculated modal transmission of the taper for a narrowing of the fiber diameter from 125 to 10 μm as a function of the taper length. Modes with radial symmetry are mainly involved in a conical transition.

Table 1
Propagation constants and related beating lengths for the two main modes HE_{11}, HE_{12} in the micro-fiber for three different diameters and for two different external substances: air and methanol.

	Power (%)		β air (μm^{-1})		β methanol (μm^{-1})		L_b (μm)		
Width (μm)	HE_{11}	HE_{12}	HE_{11}	HE_{12}	HE_{11}	HE_{12}	Air	Methanol	$L_{b\text{-air}}/L_{b\text{-methanol}}$
10	63	33	5.918	5.796	5.920	5.810	51.7	57.0	0.91
15	64	31	5.935	5.890	5.936	5.893	137.7	145.7	0.94
20	67	30	5.940	5.916	5.940	5.917	260.5	271.2	0.96

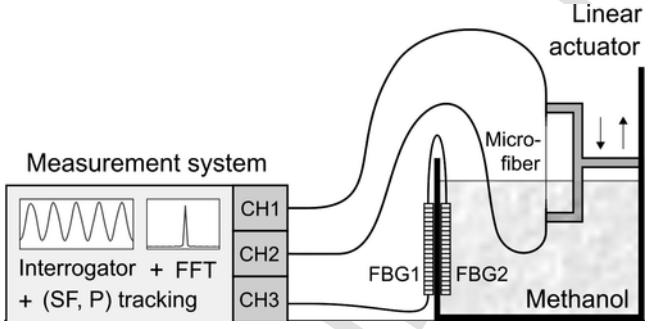

Fig. 3. Experimental setup for the liquid level tests. The linear actuator immerses the micro-fiber in the methanol tank. The measurement system calculates in real time the spatial frequency and phase of the spectral response of the sensor.

2. Sensors design

The sensing transducers are based on biconical optical fiber tapers (OFTs) (see Fig. 1). We fabricated the tapers using standard communication single-mode fibers that were narrowed from its nominal diameter of 125 μm down to a micro-wire of several micrometers wide and 40 mm long. A Taper Manufacturing Station (TMS, 3SAE from NorthLab Photonics) was employed to fabricate the OFTs. This fiber tapering system operates in partial vacuum which is advantageous providing low loss and great repeatability [28]. The tolerance results are mainly dictated by fiber preparation rather than the TMS performance. The scanned waist diameters of a 125 μm fiber tapered to 62.5 or 25 μm could vary up to ± 1 μm or ~2%. In addition to this, if offers an automatic and built in taper scan function, that allows a real time check of the manufactured optical fiber taper.

Despite the reduced waist diameter of the fabricated OFTs, the micro-fiber holds tens of guided modes even for a diameter as low as 10 μm due to the high index contrast of the silica-air interface.

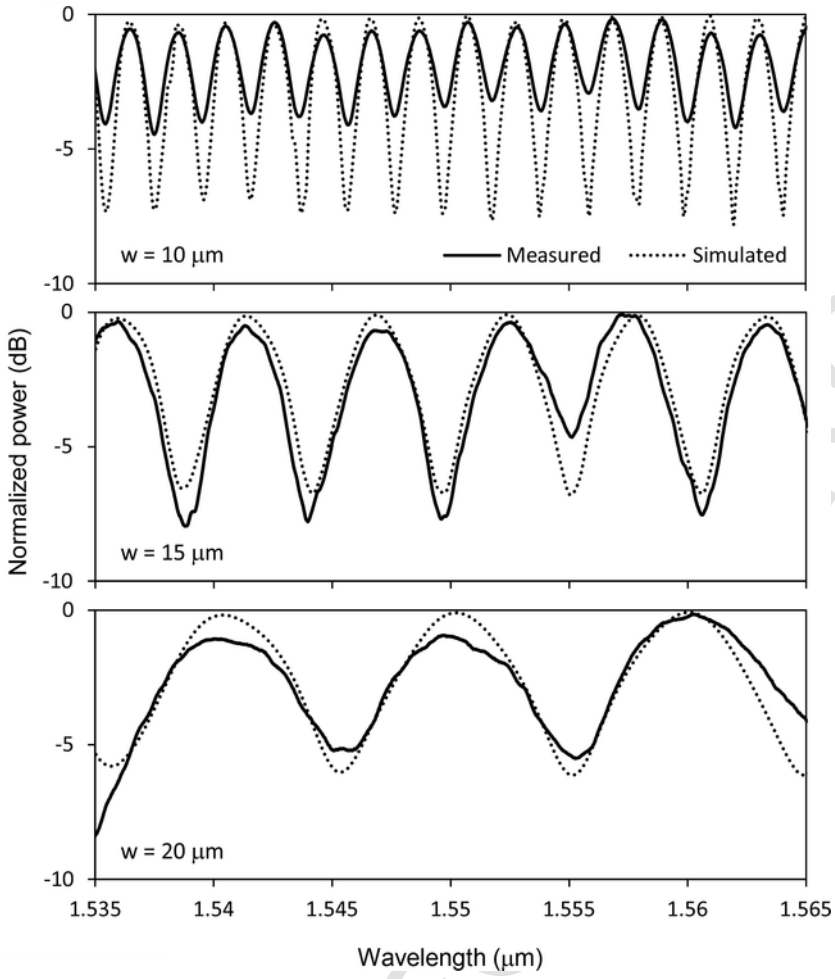

Fig. 4. Optical spectrum of the tested optical tapered fibers for three different waist diameters w = 10, 15, 20 μm.

Higher order modes extend deeper in the surrounding medium enhancing their sensitivity to refractive index changes in the environment as a result of the immersion of the micro-fiber in liquid.

The guided mode in the incoming SMF entering the first transition progressively transforms into the main guided mode of the micro-fiber. A smooth narrowing of the fiber longer than about 1 cm supposes an adiabatic transition where all the optical power remains in the fundamental mode of the waist. In such case, there would not be environment dependent intermodal interference. Therefore, a sharper tapering beyond adiabaticity has to be defined to the input taper in order to transfer optical power form the fundamental mode (HE_{11}) to the radially symmetrical second order mode (HE_{12}) minimizing the excitation of higher order modes. In this way, we obtain a clear interference pattern with a large amplitude when the micro-fiber in immersed in liquid.

A commercial fully vectorial finite difference mode solver [29] has been used for the analysis of the tapered fiber. The taper shape that better fits the transitions obtained by the fabrication station is a cosine interpolation function. Fig. 2 shows the mode power transmission as a function of the transition length for a minimum waist diameter of 10 μm. As expected in a symmetrically conical transition, radially symmetrical modes gather the optical power delivered by the fundamental mode if the adiabaticity criterion is broken down. The insets of Fig. 2 also show the intensity profiles of modes HE_{11}, HE_{12} and HE_{13}. We confirm that the fundamental mode gradually losses power as the taper shortens and that this power efficiently transfers to the mode HE_{12}. For a compromise length of 2500 μm, the mode HE_{12} reaches a 33 % of the optical power whereas the mode HE_{11} keeps a 63 %. This distribution provides an adequate amplitude in the interference pattern. The rest of the cladding modes receive less than a 4% avoiding higher frequency interferences in the measurement that would also cause crosstalk in the multiplexed scheme. Wider diameters of the central waist show slightly lower power transfer to the HE_{12} mode. A diameter of 20 μm ends up with 30 % of the input power in the HE_{12} mode in the micro-fiber.

Once the two main modes in the micro-fiber are excited, they experiment a periodic interference during propagation. Due to the reduced diameter of the waist, there is a considerable influence of the external material on the propagation and the interference of these modes. Table 1 shows the propagation constants of modes HE_{11} and HE_{12} for three different diameters and for two different external substances used in the level measurement tests (air and methanol). Corresponding modal power distribution induced by the tapered fiber and the beat lengths of the bimodal interferences are also shown. We see that the interference length of the main modes decreases substantially for smaller fiber diameters, but that the relative difference between beat lengths in air and liquid increases, which implies higher spatial frequencies and sensitivity.

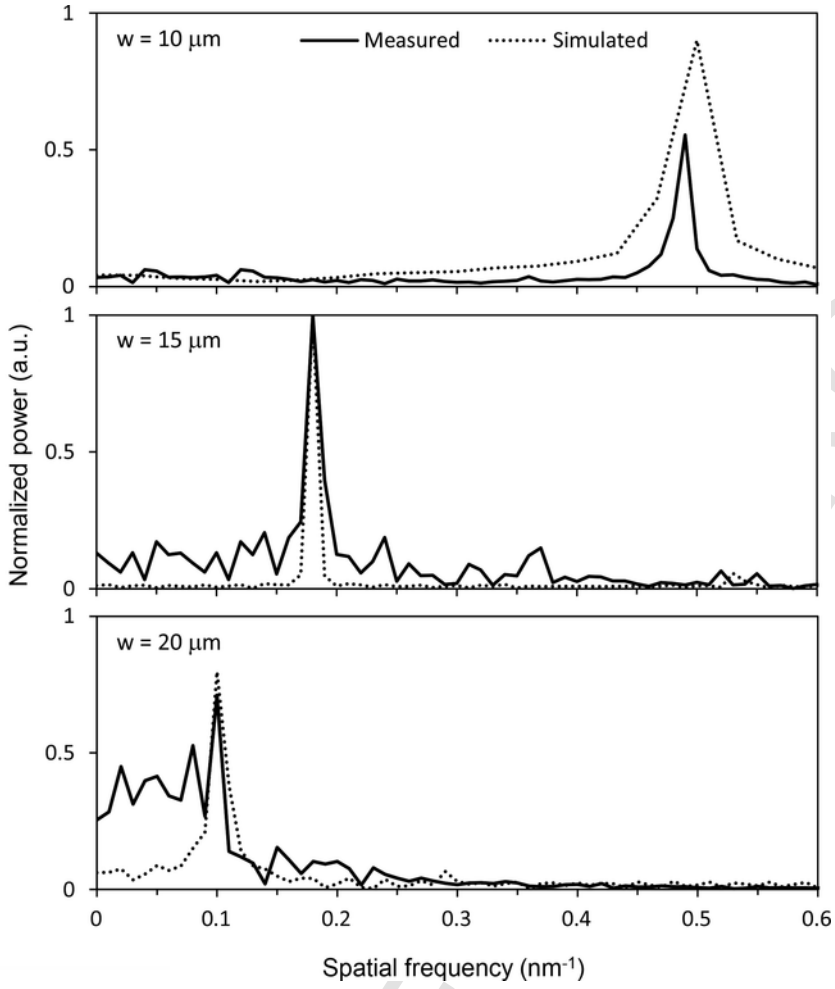

Fig. 5. Normalized magnitude of the FFT of the optical response of the micro-fibers for three different waist diameters w = 10, 15, 20 μm.

3. Fabrication and experimental setup

The biconical non-adiabatic tapered fibers and the 40 mm-long micro-fibers were fabricated by heating the SMF with a thermally stabilized plasma in partial vacuum and applying a precise tension on both sides of the fiber. A microscopic vision system monitors the evolution of the width of the structure. This scheme results in a high quality, low loss and good repeatability tapering procedure [30].

Fig. 3 illustrates the experimental set up for the liquid level sensitivity tests. The tank was filled with methanol (NCAS: 67−56-1) for the immersion tests. The refractive index of the liquid is 1.3172 at 1.55 μm [31]. Two fiber optic Bragg gratings (FBG) were glued to both sides of the wall of the container for temperature evaluation. The C-shaped element holding the micro-fiber was made with glass in order to minimize the influence of the thermal expansion. The ends of the biconical tapered fibers were pre-strained using a 20 g load before gluing to the support to avoid undesired non-linear responses during tests. The linear actuator precisely governs the immersion depth, as well as its speed.

The measurement of the immersion depth of the tapered micro-fiber is based on the frequency and phase changes of the transmission interference pattern as a function of the liquid level. We obtain the fringes of the sensor in the optical spectrum using a commercial optical interrogator, Micronoptics Si155 [32] that offers a wavelength resolution of 10 pm and a wavelength accuracy of 1 pm for a 100 nm range. Then, we perform a real time calculation of the FFT of this spectrum and track the spatial frequency and phase of the main spectral component to obtain precise information of the measured parameter. The use of the FFT phase-based demodulation instead of conventional techniques (such as monitoring a peak/valley of the spectrum) allows achieving a higher effective resolution [33].

In this setup, channels one and two of the interrogator measure the transmission response of the sensor, whereas channel three quantifies the reflected wavelengths from the FBGs for temperature sensing. If necessary, these FBGs could be connected to the same fiber channel of the level sensor in a simpler scheme.

4. Results and discussion

Fig. 4 shows the measured optical transfer function in air of the micro-fibers for three diameter waists of 10, 15 and 20 μm. The patterns reveal a clean and regular interference suggesting an effective power transference from the main mode to the second order cylindrical mode. Power leakage to higher order modes in the tapered fiber would imply irregular and noisy fringes in the optical spectrum. The amplitude of the obtained signals ranges between 4 and 8 dB, slightly lower than the calculated values but still confirming a significant accumulation of optical power by mode HE_{12} (see also Table 1).

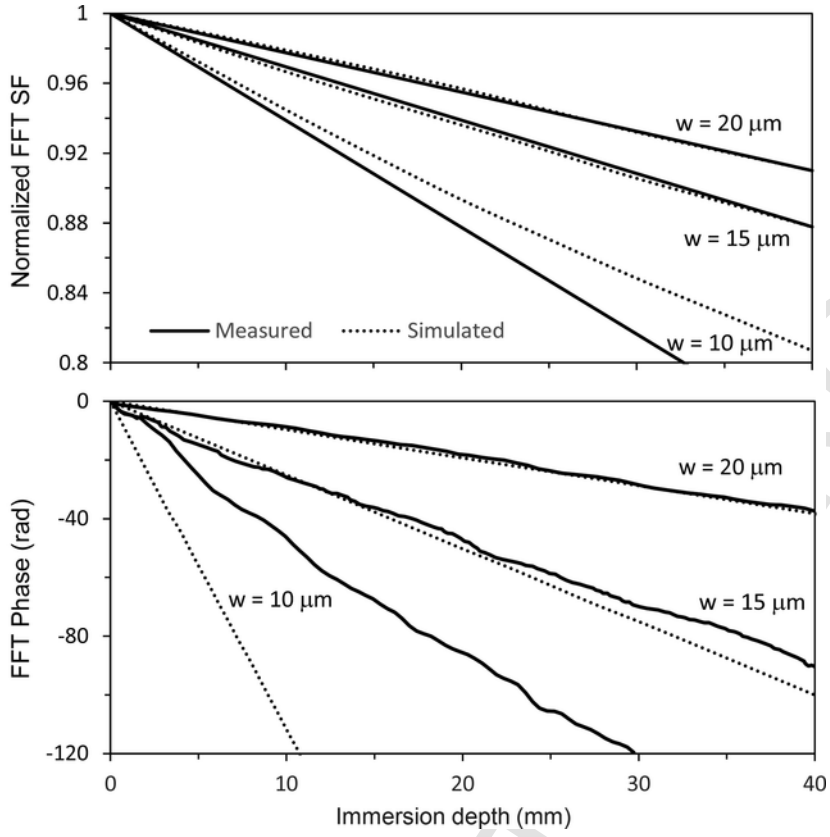

Fig. 6. Normalized spatial frequency (SF) and phase evolution of the three micro-fibers as a function of the immersion depth in methanol.

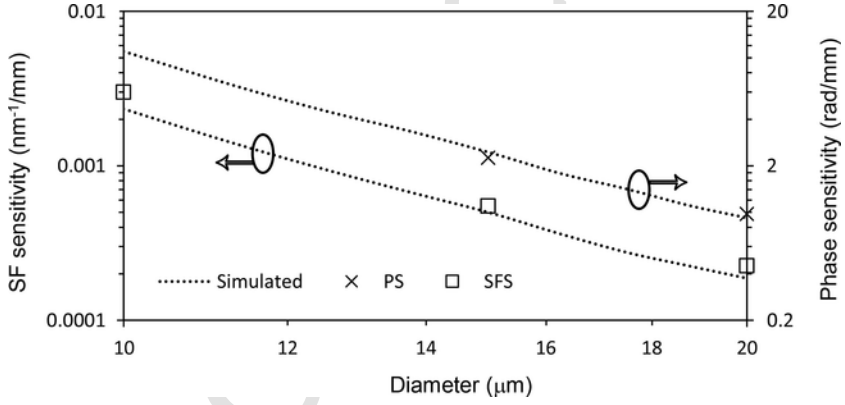

Fig. 7. Measured and calculated SF and phase sensitivity as a function of the micro-fiber width.

Smaller diameters mean bigger differences in the propagation constants between modes that at the same time imply shorter beat lengths. Therefore, the biconical tapered fiber is more sensitive to optical wavelength variations, showing higher interference frequencies in the pattern. These spectral frequencies, which are thoroughly tuned by the width of the micro-fiber, is the basis to multiplex several sensors into the same optical channel of the interrogator, as it is shown in the last section of this work. The normalized magnitude of the FFT of each interference pattern is shown in Fig. 5. The spatial frequencies of the main spectral components are 0.47, 0.18 and 0.10 nm^{-1}.

Interferometric sensors are generally limited to relative measurements. The measuring process is phase-based, and measurements are referred to an initial position from which we track accumulative variations in successive periods [12]. In order to avoid this limitation, we trace the absolute position of the peak in the spatial frequency spectrum together with its phase as the micro-fiber immerses in liquid. Fig. 6 shows the normalized spatial frequency (SF) and phase evolution of the peak of each sensor as a function of the immersion depth. Note that a simple interpolation has been used in the calculation of the peak position for the case of the spatial-frequency variation.

As expected, slimmer diameters experience larger variations in both parameters. We remark the excellent linearity of the frequency measuring confirming its potential to analyze this kind of sensors. Measured values adequately fit results predicted by simulations, except for the phase progression of the smaller waist where theoreti-

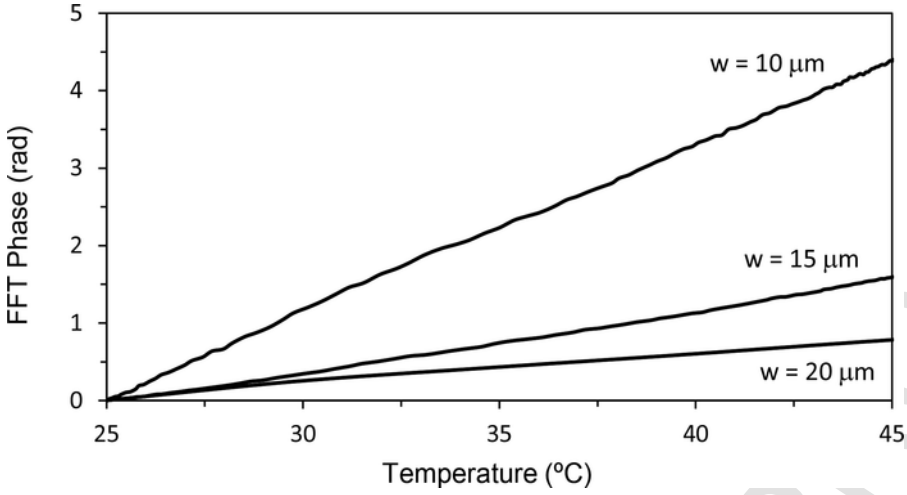

Fig. 8. Phase trace during the temperature test for each sensor.

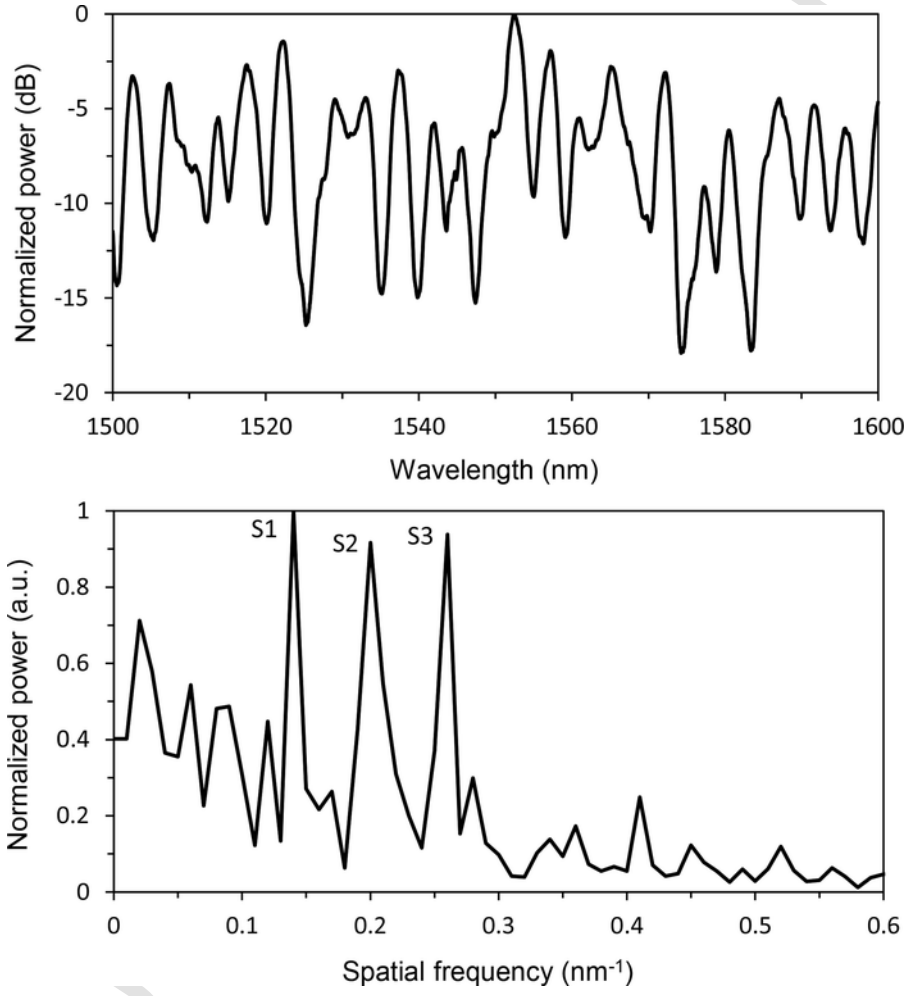

Fig. 9. a) Optical spectrum results for the three sensors placed in series. b) FFT magnitude of this optical spectrum.

cal calculations show a much higher sensitivity than measurements: 11.4 versus 3.7 rad/mm. The technical issue shown up next clarifies this mismatch. The predicted sensitivity implies that we get an advancement of 2π radians in the phase for a displacement of only 0.55 mm in the immersion depth. Since the step of the linear actuator during the measurement was 0.4 mm, we are registering aliased information from a periodic signal. Therefore, we are not retrieving real information due to the huge sensitivity of the smaller micro-fiber.

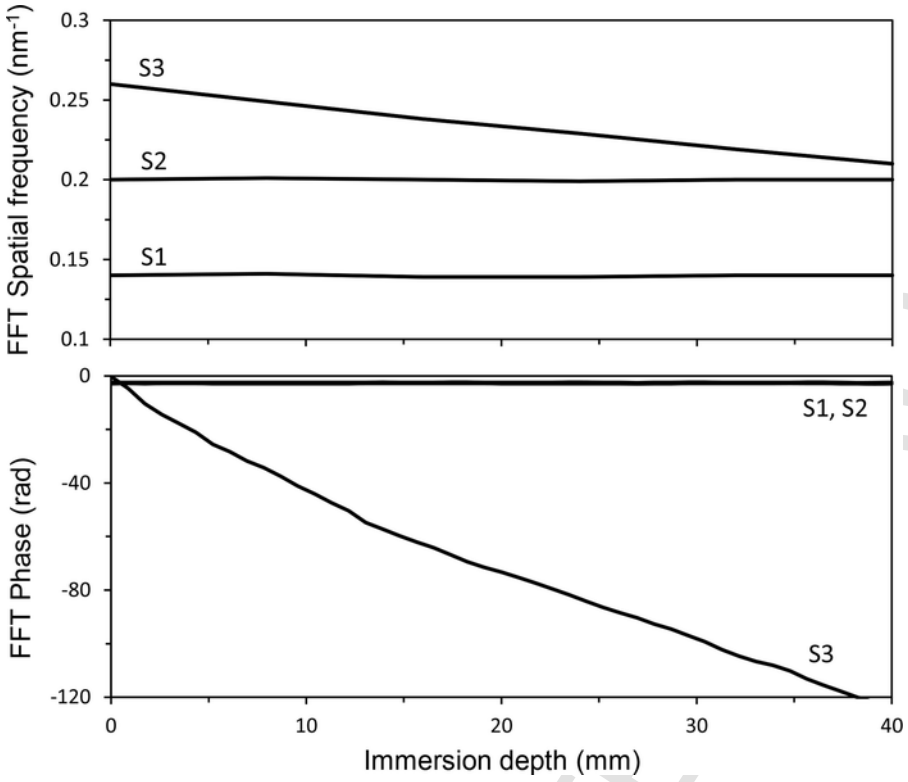

Fig. 10. SF and phase evolution of the multiplexed three sensors during the immersion of sensor S3.

Writing down the measured and calculated sensitivity values of the SF and phase as a function of the considered three diameters, we obtain the graph shown in Fig. 7. The aliased phase measurement for 10 μm has been removed. The phase sensitivity oscillates between 11.4 rad/mm (theoretical calculation) for the thinner fiber and 0.97 rad/mm for the widest; whereas the SF varies between 3 and 0.23 pm^{-1}/mm, respectively. The multiplexing of sensors over different spatial frequencies fabricating them with so many other diameters implies having diverse sensitivities for each one of them varying in the range of one order of magnitude.

In order to evaluate the behavior of the micro-fibers under temperature variations, we have tested newly fabricated specimens in a climatic chamber [34]. Inducing a temperature alteration of 20 °C, we have registered the evolution in the SF and phase of each sensor. The recorded temperature sensitivity is much lower than the variation induced by the immersion depth. In the worst case, which corresponds to one with 20 μm width, a temperature variation slightly higher than 20 °C is needed to generate an uncertainty of 1 mm in the liquid level value. Fig. 8 shows the phase displacement results for temperature variations for the three micro-fiber diameters.

Regarding the error of the measurements, the mechanical setup is the main error source. Both the linear actuator inaccuracy and the C-shaped support for the taper without a proper packing, make vibrations an important source of mismatch between measured and real values. Upgrades in the mechanical setup and a proper sensor packaging would improve the results. Compared to the error induced by the mechanical setup itself, other errors induced in the fabrication process or by the optical interrogator, can be considered negligible (after an adequate calibration of the sensor sensitivity).

5. Sensor multiplexing

In order to examine and validate a multiplexed sensor system based on the division of the SF of the optical spectrum, we fabricated three new biconical tapers and micro-fibers: S1, S2 and S3. Respective values of 17, 14.5 and 13 μm for the diameters of the micro-fibers provided sufficiently separated spectral components avoiding crosstalk during the peak drift in the immersion. We placed the sensors in series and connected to the same input and output interrogator channels previously used in the characterization of single sensors. Fig. 9a) shows the optical spectrum response of the set of sensors distributed in series, and Fig. 9b) shows its FFT magnitude calculation result. The main peak for each sensor in the FFT spectrum were located at 0.14, 0.20 and 0.24 nm^{-1}.

The validation of the multiplexing system was fulfilled by exciting one of the sensors with a progressive immersion keeping the rest unexcited out of the liquid recipient. Fig. 10 shows the tracked SF and phase of the three sensors in the immersion test of S3. Results evidence a good performance of the multiplexing scheme with a maximum crosstalk of 0.2 rad/mm between sensors. Sensors showed phase sensitivities of 1.2, 1.7 and 3 rad/mm, and SF sensitivities of 0.25, 0.5 and 1.25 pm^{-1}/mm.

6. Conclusion

The multiplexing of several liquid level optical sensors is proposed and experimentally demonstrated. Transducers are based on the bimodal interference of the main cylindrical guided modes in optical micro-fibers obtained by the biconical tapering of standard SMF. The shape and length of the tapering is designed in order to provide an effective and efficient power transfer between the guided core mode

of the SMF and the cylindrical second order mode in both tapered fibers. The measurement of the immersed tapered fiber is realized by first interrogating the sensor to obtain the optical spectrum of the bimodal interferences, then calculating its FFT in real time and finally tracking the SF and phase of the main peaks. Simulations have been performed to fully characterize the sensors sensitivity to the spatial frequency and phase as a function of the width of the micro-fiber, the most sensitive parameter in the system. Micro-fibers with the lowest diameters present phase sensitivities as high as 11.4 rad/mm. The SF domain is finally used to multiplex three sensors with different waist diameters in the same channel of the interrogator. Low crosstalk and the predicted sensitivities are obtained for each sensor. The proposed system disposes additional channels in the interrogator that could be used for the compensation of the effect of temperature if needed.

Funding

This work was supported by the Spanish Agencia Estatal de investigación within projects TEC2016-76021-C2-1-R, and UNPN15-EE-3167, by the FEDER funds of EU and by the Institute of Smart Cities by means of a postdoctoral fellowship.

CRediT authorship contribution statement

Marko Galarza: Conceptualization, Methodology, Validation, Formal analysis, Investigation, Data Curation, Writing - original draft, Writing - review & editing, Visualization. **Rosa Ana Perez-Herrera:** Methodology, Validation, Formal analysis, Investigation, Writing - review & editing, Visualization. **Daniel Leandro:** Methodology, Validation, Formal analysis, Investigation, Writing - review & editing, Visualization. **Aitor Judez:** Validation, Formal analysis, Investigation. **Manuel López-Amo:** Conceptualization, Methodology, Validation, Formal analysis, Resources, Writing - review & editing, Visualization, Supervision, Project administration, Funding acquisition.

Declaration of Competing Interest

None.

References

[1] E. Frederick, A. Lateef, K. Olufemi, O. Abdulmutolib, J. Anifowose, Overview of liquid level detection technologies with performance characteristics assessment and energy cost saving for household water pumps, WWJMRD 3 (September 9) (2017) 287–294.
[2] C.A.R. Díaz, et al., Optical fiber sensing for sub-millimeter liquid-level monitoring: a review, IEEE Sens. J. 19 (September 17) (2019) 7179–7191.
[3] A.G. Leal-Junior, C. Marques, A. Frizera, M.J. Pontes, Multi-interface level in oil tanks and applications of optical fiber sensors, Opt. Fiber Technol. 40 (2018) 82–92.
[4] O.S. Wolfbeis, Fiber-optic chemical sensors and biosensors, Anal. Chem. 78 (12) (2006) 3859–3874.
[5] C. Hillman, k. Rogers, M. Pecht, R. Dusek, A. Dasgupta, B. Lorence, Solder failure mechanisms in single-sided insertion-mount printed wiring boards, Circuit World 25 (September 3) (1999) 23–28.
[6] P. Li, Y. Cai, X. Shen, S. Nabuzaale, J. Yin, J. Li, An accurate detection for dynamic liquid level based on MIMO ultrasonic transducer array, IEEE Trans. Instrum. Meas. 64 (March 3) (2015) 582–595.
[7] F.N. Toth, G.C.M. Meijer, M. VanderLee, A new capacitive precision liquid-level sensor, In: Presented at 20th Biennial Conference on Precision Electromagnetic Measurements, Braunschweig, Germany, 1996, pp. 356–357.
[8] K. Yamada, K. Watanabe, Liquid-level sensing by a cylindrical piezoelectric resonator operating in a trapped-energy mode, In: Presented at Joint Conference of the European Frequency and Time Forum and IEEE International Frequency Control Symposium, Besancon, 2017, pp. 647–648.
[9] G. Zheng, H. Zong, X. Zhuan, J. Luan, Fast dynamic liquid level sensor based on liquid resistance, In: Windhoek, South Africa, Presented at AFRICON 2007, 1-6, 2007.
[10] S. Chakravarthy, R. Sharma, R. Kasturi, Noncontact level sensing technique using computer vision, IEEE Trans. Instrum. Meas. 51 (April 2) (2002) 353–361.
[11] X. Zhang, W. Peng, Z. Liu, Z. Gong, Fiber optic liquid level sensor based on integration of lever principle and optical interferometry, IEEE Photonics J. 6 (April 2) (2014) 1–7.
[12] E. De la Rosa, L.A. Zenteno, A.N. Starodumov, D. Monzon, All-fiber absolute temperature sensor using an unbalanced high-birefringence Sagnac loop, Opt. Lett. 22 (April 7) (1997) 481–483.
[13] C.A.F. Marques, G.-D. Peng, D.J. Webb, Highly sensitive liquid level monitoring system utilizing polymer fiber Bragg gratings, Opt. Express 23 (March 5) (2015) 6058–6072.
[14] C.A.F. Marques, A. Pospori, D.J. Webb, Time-dependent variation of POF Bragg grating reflectivity and wavelength submerged in different liquids, Opt. Laser Technol. 94 (September) (2017) 234–239.
[15] J.Y. Dong, S. Xiao, H. Xiao, J. Liu, C. Sun, S. Jian, An optical liquid-level sensor based on D-shape fiber modal interferometer, IEEE Photonics Technol. Lett. 29 (July 13) (2017) 1067–1070.
[16] J.E. Antonio-Lopez, J.J. Sanchez-Mondragon, P. LiKamWa, D.A. May-Arrioja, Fiber-optic sensor for liquid level measurement, Opt. Lett. 36 (September 17) (2011) 3425–3427.
[17] D. Wang, Y. Zhang, B. Jin, Y. Wang, M. Zhang, Quasi distributed optical fiber sensor for liquid level measurement, IEEE Photonics J. 9 (December 6) (2017) 1–7.
[18] S.F. Knowles, B.E. Jones, S. Purdy, C.M. France, Multiple microbending optical-fibre sensors for measurement of fuel quantity in aircraft fuel tanks, Sens. Actuators A Phys. 68 (December) (1998) 320–323.
[19] J.A. Morris, C.R. Pollock, A digital fiber-optic liquid level sensor, J. Lightwave Technol. 5 (1) (1987).
[20] P. Datta, I. Matías, C. Aramburu, A. Bakas, M. López-Amo, J.M. Oton, Tapered optical-fiber temperature sensor, Microw. Opt. Technol. Lett. 11 (February 2) (1996) 93–95.
[21] F.J. Arregui, I.R. Matias, C. Bariain, M. Lopez-Amo, Experimental design rules for implementing biconically tapered single mode optical fibre displacement sensors, In: European Workshop on Optical Fibre Sensors, SPIE Proceedings, vol. 3483, 1998, pp. 164–169, June.
[22] T. Wei, X. Lan, H. Xiao, Fiber inline core–cladding-mode Mach–Zehnder interferometer fabricated by two-point CO2 laser irradiations, IEEE Photonics Technol. Lett. 21 (May 10) (2009) 669–671.
[23] Z. Tian, S.S.-H. Yam, In-line single-mode optical fiber interferometric refractive index sensors, J. Lightwave Technol. 27 (July 13) (2009) 2296–2306.
[24] L. Chen, et al., Label-free fiber-optic interferometric immunosensors based on waist-enlarged fusion taper, Sens. Actuators B Chem. 178 (2013) 176–184.
[25] P. Niu, J. Zhao, C. Zhang, H. Bai, X. Sun, J. Bai, Reflective intensity-demodulated refractometer based on S Fiber taper, IEEE Photonics Technol. Lett. 30 (1) (2018) 55–58.
[26] D. Leandro, M. Bravo, A. Ortigosa, M. Lopez-Amo, Real-time FFT analysis for interferometric sensors multiplexing, J. Light. Technol. 33 (January 2) (2015) 354–360.
[27] A. Judez, D. Leandro, R.A. Pérez-Herrera, M. Galarza, M. Lopez-Amo, High sensitivity fiber-optic liquid level sensor using biconical tapered fibers, In: 26th International Conference on Optical Fibre Sensors, Proc. of OFS 26, Paper TuE45, Sep, 2018.
[28] Taper Manufacturing Station (TMS), SAE Technologies, 2019, [Online] Available: https://www.3sae.com/products/3saetapermanufacturingstation.php. [Accessed July 29, 2019].
[29] FIMMWAVE/FIMMPROP, Photon Design Ltd., 2019, [Online] Available: http://www.photond.com. [Accessed July 29, 2019].
[30] 3SAE Taper Manufacturing Station (TMS), SAE Technologies Inc., 2019, [Online] Available: https://www.3sae.com. [Accessed July 29, 2019].
[31] K. Moutzouris, M. Papamichael, S.C. Betsis, I. Stavrakas, G. Hloupis, D. Triantis, Refractive, dispersive and thermo-optic properties of twelve organic solvents in the visible and near-infrared, Appl. Phys. B 116 (2013) 617–622.
[32] Optical Sensing Instrument si155, Micron Optics Inc., 2019, [Online] Available: https://www.micronoptics.com. [Accessed July 29, 2019].
[33] D. Leandro, M. Bravo, M. Lopez-Amo, High resolution polarization-independent high-birefringence fiber loop mirror sensor, Opt. Express 23 (24) (2015) 30985–30990.
[34] FED 115, BINDER GmbH, 2019, [Online] Available: https://www.binder-world.com. [Accessed July 29, 2019].

Marko Galarza received the Telecommunications Engineering degree from the Universidad Pública de Navarra, Spain, in 1997 and the Ph.D. degree from the same university and University of Ghent, Belgium, in 2003. In 2004, he was a visiting postdoctoral researcher

at the Photonics Research Group, Ghent University−IMEC, Ghent, Belgium, supported by a Marie Curie fellowship. In 2005, he joined the Optical Communications Group, Department of Electrical, Electronic and Communication Engineering, Universidad Pública de Navarra as an Assistant Professor. His research interests are fiber-optic sensors and integrated optics components, such as semiconductor waveguides, laser diodes and microring resonators.

Rosa Ana Perez-Herrera received the Telecommunications Engineering degree from the University of Cantabria, Santander, Spain, in 2004 and the Ph.D. degree from the Universidad Pública de Navarra, Pamplona, Spain, in 2010. In 2005, she joined the Optical Communications Group, Department of Electrical and Electronic Engineering, Universidad Pública de Navarra. During this period, she was a visiting Ph.D. student at City University of London and Parma University, Italy, among others. In 2009, she became an Assistant Professor at Universidad Pública de Navarra. Her research interests are in Raman amplifiers, erbium-doped amplifiers, fiber-optic sensors, and multiplexing architectures.

Daniel Leandro was born in Lumbier, Spain, in November 1984. He received the Telecommunication Engineering degree, the Communication Master's degree, and the Ph.D. degree from the Universidad Pública de Navarra, Pamplona, Spain, in 2010, 2012, and 2016, respectively. He has been a visiting Ph.D. student in the School of Engineering and Mathematical Sciences, City University of London, London, U.K. In 2012, he joined the Optical Communications Group, Department of Electrical, Electronic and Communication Engineering, Universidad Pública de Navarra. His research interests include fiber optic lasers, interferometric sensor systems, fiber sensor networks, and multiplexing architectures.

Aitor Júdez received the Automatic and Industrial Electronics Engineering degree from the University of the Basque Country, Spain, in 2011. He is currently working toward the Ph.D. degree in communication technologies, bioengineering and renewable energies at Universidad Pública de Navarra. His research interests are fiber-optic sensors, photonic crystal fibers, micro-fibers, fiber-optic lasers, and optical interrogation.

Manuel López-Amo is full-professor in photonics at Universidad Pública de Navarra (UPNA, Spain) since 1996. He is the head of the Optical Communications group of that University. His research interests are in optical fiber sensors, optical networks, optical fiber lasers, semiconductor lasers and integrated optics. He is the author of more than 300 JCR peer reviewed technical articles and international conferences. He has led 31 research projects being co-investigator in another 26. He is the Spanish representative at the experts committee IEC SC86C WG2 on Fiber Optic Sensors, and the European Cost Actions TD1001 "OFSeSa" and 299 "Fides". He has been an Associate Editor at IEEE/OSA Journal of Lightwave Technology and at MDPI Sensors among others. He is a senior member of IEEE and member of the OSA.